PHILOSOPHICAL MAGAZINE A, 1996, VOL. 74, NO. 5, 1235–1244

Inert strength of subthreshold and post-threshold Vickers indentations on fused silica optical fibres

By B. LIN and M. J. MATTHEWSON

Fiber Optic Materials Research Program,
Department of Ceramics, Rutgers University, Piscataway,
New Jersey 08855-0909, USA

[*Received in revised form 5 July 1996*]

ABSTRACT

The strength of Vickers indentations made in air on fused silica optical fibres has been studied with indentation loads in the range 5 mN–20 N which spans the threshold region for radial crack formation. Handling and strength-testing techniques are described which permit measurements to be made in this strength range that is intermediate between 'pristine' and post-threshold. The results of inert strength measurements (i.e. made in liquid nitrogen) are compared with existing models for the behaviour of subthreshold and post-threshold indentations and reasonable agreement is found between experiment and theory if it is assumed that the true threshold (i.e. for indentations performed in an inert environment) is substantially higher than observed for indents made in air. The experimental results are somewhat stronger than previously published data and this is at least partially attributed to the latter not employing a completely inert test environment.

§ 1. INTRODUCTION

The strength of fused silica optical fibre specimens of length about 1 m is usually high with a narrow distribution reflecting the pristine 'flaw-free' intrinsic strength of the glass surface (Kurkjian and Paek 1983). However, for lengths of about 100 m or more, a broad low-strength mode may appear owing to the presence of occasional weak defects. These defects may adversely affect the mechanical reliability of the fibre if it is subjected to mechanical stress at any stage of its lifetime since the defect can grow because of attack by environmental moisture (fatigue), leading to delayed failure (Gulati 1992). These weak defects are extrinsic in nature and may arise from handling or abrasion damage which may occur during manufacturing, cabling, installation or repair. Another common source of defect is particles which can adhere to the fibre surface during the drawing process. The most severe defects can be removed by proof testing, but any surviving defects or defects introduced after proof testing are a concern for fibre reliability.

The behaviour of weak defects is difficult to study directly owing to their scarcity along the fibre length. Therefore reliability is typically estimated using the subcritical crack growth model (Wiederhorn 1972) which considers the fatigue (stress corrosion) of a sharp residual stress-free crack under the combined influence of moisture and applied stress. The fatigue parameters of weak fibres are then assumed to be similar to those measured for short lengths of pristine material (Griffioen 1994). Such an approach is hard to justify since neither type of fibre is adequately described by Wiederhorn's model; pristine fibre is thought to be flaw free (Kurkjian and Paek

0141–8610/96 $12 · 00

1983) while weak defects generally do not show well-defined cracks. Also, weak defects are often associated with intense residual stress fields which are caused mechanically by abrasion, or thermally in the case of surface adhering particles which have substantial thermal expansion mismatch with the low-expansion silica.

An alternative approach for studying weak flaws is to introduce defects artificially in large numbers, and many techniques have been employed. For example, the fibre may be abraded after drawing (Glaesemann 1992) or the fibre preform can be deliberately contaminated with surface particles (Breuls and Svensson 1993). While such techniques are relatively convenient because they produce large quantities of uniformly weakened fibre, they suffer the significant disadvantage that it is not possible to control the resulting strength to any great extent. In this work we use Vickers indentations to model possible behaviour of weak fibre. This technique is particularly useful since the residual strength can be controlled over a wide range by varying the indentation load.

Dabbs and Lawn (1985) observed that, while radial cracks form at the indentation corners at high loads, radial cracks are not formed below some threshold load. They found that the residual strength of subthreshold and post-threshold indents do not follow the same trends with the presence of radial cracks causing post-threshold indents to be discontinuously weaker than subthreshold indents. The most severe flaws expected in typical proof-tested optical fibre have strengths corresponding to subthreshold indents. Most work on indentations has concerned the post-threshold regime since most materials are substantially weaker than optical fibre. The only available subthreshold data for fused silica are due to Dabbs and Lawn (1985) and Jakus *et al.* (1988) but their data only span a narrow range of loads (150–680 mN) which does not overlap the post-threshold region (about 10 N and above). The data therefore neither characterize subthreshold behaviour in detail nor provide a sensitive test of subsequently developed fracture mechanics models (Jakus *et al.* 1988, Choi, Ritter and Jakus 1990, Lathabai, Rödel, Dabbs and Lawn 1991). The reason for the narrow range of data was the unavailability of suitable test techniques; post-threshold data were for indented rods broken in four-point bending while almost all the subthreshold measurements were for indented optical fibre broken in uniaxial tension. These techniques do not make the threshold region readily accessible. Also, tension cannot be used for very low loads since failure occurs preferentially at damage produced on the rear surface of the specimen where it is supported during indentation. Baikova, Pukh and Talalakin (1974) and Aslanova *et al.* (1982) present data for indentation on HF-etched silica surfaces. Their data roughly agree with those of Dabbs and Lawn (1985) and Jakus *et al.* (1988) but it is not clear what test environment they used.

In this paper we present strength data for indentations in the load range 5 mN–10 N. While extending the subthreshold data to much lower loads, the threshold region is also covered. New handling and testing techniques have been developed in order to achieve this and they are described. The data are used to examine critically the existing fracture mechanics models for the subthreshold behaviour.

§ 2. Experimental details

Bending techniques are used throughout this work to prevent premature failure at the fibre rear surface which might have been damaged where it is supported during indentation. No single bending technique can conveniently span the entire strength range of interest. Therefore two-point bending (Matthewson, Kurkjian and Gulati

1986) is used to measure higher strengths while a novel miniaturized four-point bend test (Nelson, Matthewson and Lin 1996) is used for the lower strengths. For a given fibre diameter, these two techniques do not necessarily overlap. Therefore the two-point bending measurements were made using fibre of 100 μm diameter while fibre of 1000 μm diameter was used in four-point bending. In the region of overlap these two techniques give similar results (Nelson *et al.* 1996). Intermediate fibre diameters have also been used and no diameter dependence of the indentation behaviour has been observed. Strength and fatigue behaviour of unindented fibre has also been found to be independent of fibre diameter in the range 70–1000 μm (B. Lin, M. J. Matthewson and C. R. Kurkjian 1995, unpublished work). It is important to note that the overlap between these two test techniques does not coincide with a critical region of indentation behaviour; in the earlier work, different techniques were used on either side of the threshold region.

All indentations were performed on bare fused silica fibre after removing the polymer protective coating by briefly immersing in hot (about 200°C) sulphuric acid. This stripping method does not affect the fibre strength (Matthewson, Kurkjian and Hamblin 1996). A microhardness tester equipped with a Vickers diamond pyramid indenter was used with the peak indentation load maintained for 10 s, with available loads ranging from 2 mN to 20 N. All indentations were performed in ambient laboratory air (20–25°C; 20–50% humidity).

Samples were selected randomly from along the fibre length to avoid any systematic variation in properties. After stripping, each specimen was indented and the indentation diagonal $2a$ and radial crack length $2c$ (if present) were measured. The fibre was then broken in either the two- or four-point bend apparatus with the indent on the tensile side of the bend. To aid in alignment, a stiff paper 'flag' was attached to the end of each specimen. The flag was allowed to hang under gravity both under the indenter and in the four-point bend apparatus, so that the indent is automatically aligned upwards. In two-point bending, the fibre is inserted bent and automatic alignment is not possible; however, the flag does aid in identifying the azimuthal position of the indent. Axial alignment was made by carefully positioning the indent symmetrically between the loading pins (four-point bending) or face plates (two-point bending). Residual alignment errors have been estimated to be negligible.

The fibres were broken while immersed in liquid nitrogen (77 K) in order to eliminate stress corrosion by environmental moisture. The bending techniques used here are particularly useful for this since the fibre is readily immersed in the liquid; tensile testing cannot be performed conveniently in liquid nitrogen.

§ 3. Fracture mechanics models

There exist several fracture mechanics models in the literature for both subthreshold and post-threshold indentations and these will be compared with the experimental results. These models are briefly reviewed here.

3.1. *Post-threshold model*

Post-threshold behaviour has been widely studied and is now well understood. Marshall and Lawn (1980) model the post-threshold radial cracks as a half-penny crack and treat the residual stress as a point force opening the crack where the force χP is assumed to be proportional to the indentation load P. The total stress intensity factor for both the residual stress and applied stress σ_a is given by

$$K = \psi\sigma_a c^{1/2} + \frac{\chi P}{c^{3/2}}, \tag{1}$$

where ψ is the dimensionless crack shape parameter. Equation (1) has a minimum so that at low applied stresses the radial crack is stable. As the stress is increased, the minimum K exceeds the critical stress intensity K_c and unstable crack growth leads to failure at a stress given by

$$\sigma_f = \left(\frac{27K_c^4}{256\chi\psi^3 P}\right)^{1/3}. \tag{2}$$

At equilibrium, for a given material and flaw geometry, the right-hand side of eqn. (2) is constant so that a $\log\sigma$–$\log P$ plot is predicted to have a slope of $-\frac{1}{3}$.

3.2. *Subthreshold models*

3.2.1. *The Jakus–Ritter–Choi–Lardner–Lawn subthreshold model*

Jakus *et al.* (1988) proposed a model for the subthreshold indentations which considers the behaviour of an incipient crack and treats it as if it were a penny-shaped crack the same size as the indentation diagonal (i.e. $c = a$ where a, the half-diagonal, is related to the indentation load by $P = 2a^2H$, where H is the hardness). They then consider contributions to the stress intensity factor from tensile stresses in the surface of the plastic zone (the near-field residual stress that controls crack initiation) and the hoop tensile stress in the material outside the plastic zone (the far-field residual stress which controls crack arrest). They find two regions of behaviour. At low loads, far from the threshold, the initiation of a crack from the incipient flaw leads to spontaneous failure at a stress σ_f given by

$$\sigma_f = \frac{K_c}{\psi}\left(\frac{2H}{P}\right)^{1/4} - \frac{\Gamma}{\psi}, \tag{3}$$

where Γ is a load-independent scaling factor related to the near-field residual stress. At very low loads the term in Γ is negligible and the second term in eqn. (3) becomes negligible and the behaviour is therefore asymptotic to a straight line of slope $-\frac{1}{4}$ in a $\log\sigma_f$–$\log P$ plot. Equation (3) predicts spontaneous 'pop-in' above a critical load P_c:

$$P_c = 2H\left(\frac{K_c}{\Gamma}\right)^4. \tag{4}$$

Near the threshold, the second term of eqn. (3) becomes significant; the log–log plot curves downwards and σ_f asymptotically approaches zero at $P = P_c$. However, close to the threshold the K–c behaviour develops a second minimum which arrests the crack at some stable finite size. Further loading cause stable crack growth until K_c is again exceeded and catastrophic failure ensues. This divides the subthreshold behaviour into two regions: one where failure is initiation controlled, and one near the threshold that is propagation controlled. All published data correspond to the initiation-controlled region and the existence of the propagation-controlled subthreshold region has not been confirmed experimentally for silica. Choi *et al.* (1990) cite an approximate derivation for the strength in the propagation controlled subthreshold region as

$$\sigma_f = \left(\frac{0{\cdot}21 H K_c^4}{(\Gamma + \phi)\psi^3 P} \right)^{1/3}, \tag{5}$$

where ϕ is a load-independent scaling factor related to the far-field residual stress. A slope of $-\frac{1}{3}$ for the $\log \sigma_f$–$\log P$ plot is predicted, that is eqn. (5) is in the same form as eqn. (2) for post-threshold defects. However, Choi *et al.* do not assume that the constants are equivalent so that they predict a propagation-controlled subthreshold behaviour that is not collinear with the post-threshold behaviour.

3.2.2. *The Lathabai–Rödel–Dabbs–Lawn subthreshold model*

Lathabai *et al.* (1991) use a similar continuum cavity model to describe the residual stress distribution around the indent. However, they model the incipient flaw as a shear fault near the edge of the indent that initiates a crack at the indent corner, which is physically more reasonable. They superimpose the effect of both shear and tensile stresses on the fault and derive expressions for the subthreshold strength. However, even though their equations are substantially more complex than those of Jakus *et al.* and have more fitting parameters, the mathematical form is similar. In particular, it may be shown that at low loads the slope of the $\log \sigma_f$–$\log P$ plot asymptotically approaches $-\frac{1}{4}$ as well.

Lathabai *et al.* (1991) also derive an equation for the post-threshold strength again which is of a similar form to eqns. (2) and (5). An important difference between the Choi *et al.* and the Lathabai *et al.* models is that in the latter it is suggested that the strength in the propagation-controlled subthreshold region is governed by the same equations as in the post-threshold region, that is they are collinear. This is reasonable since the only difference between the two is whether or not an externally applied stress is required to pop in a radial crack from the first into the second minimum in the K–c curve. The failure stress required to propagate the crack out of the second minimum is not dependent on the circumstances required to propagate the crack into the minimum.

§ 4. Results and discussion

Figure 1 shows the indentation half-diagonal a and crack length c as functions of indentation load. The earlier work on subthreshold indentations did not present such data and therefore the results are compared with those of Dabbs, Marshall and Lawn (1980) for borosilicate (4% B_2O_3) fibre. The results show constant hardness throughout the range investigated (about 7 GPa). The crack lengths are similar to those of Dabbs *et al.* except that the threshold load is somewhat higher; this is to be expected given the difference in composition.

Figure 2 shows the inert strength as a function of indentation load. The 'inert' data of Jakus *et al.* (1988) and Dabb and Lawn (1985) measured in dry nitrogen gas are also shown for comparison. While all data show the same trends, the liquid-nitrogen data are systematically about 100% stronger than both the published data and our data for 20 mN indents broken in dry nitrogen. A low temperature tends to increase toughness by its effect on the elastic modulus, but this is a small effect since the room-temperature inert strength is expected to be about 90% of that in liquid nitrogen (Kurkjian, Biswas and Yuce 1966) and is insufficient to explain the difference. However, dry nitrogen is not completely inert; the strength of 20 mN indents broken in dry nitrogen gas is found to decrease about 8% as the loading rate

Fig. 1

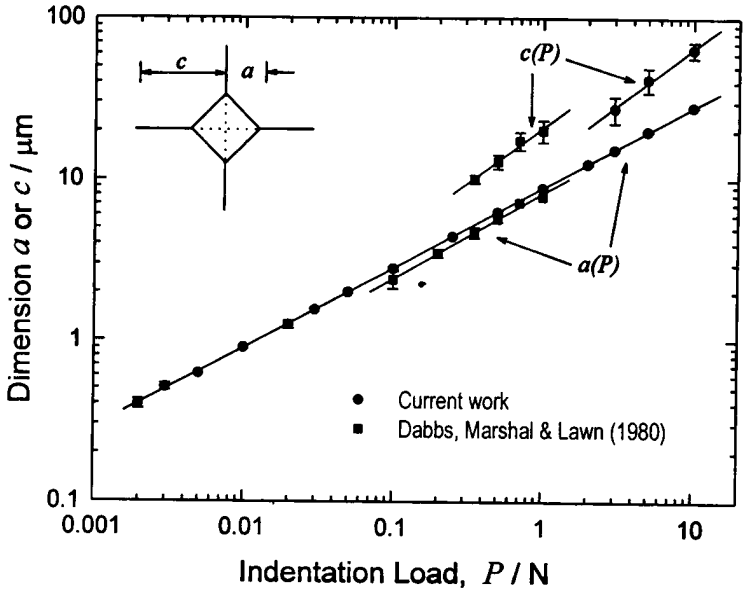

Indentation size a and radial crack length c as functions of indentation load P.

Fig. 2

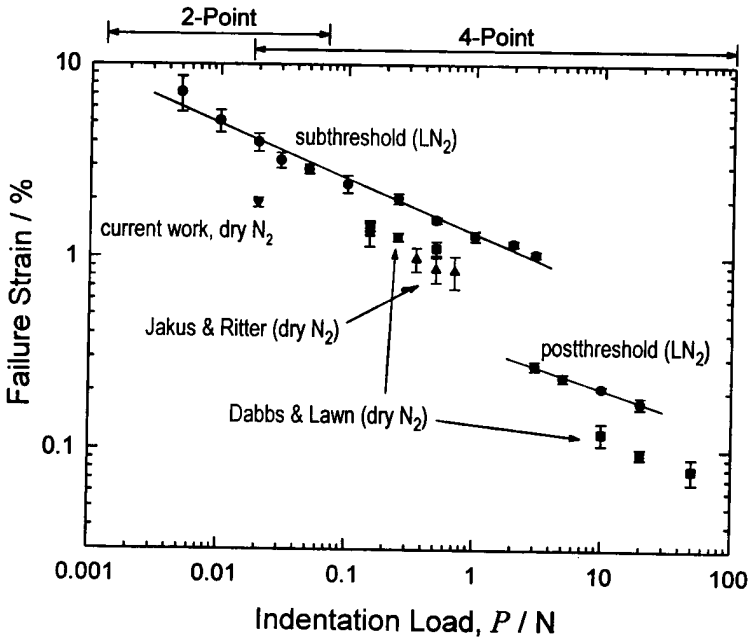

Inert (liquid-nitrogen (LN_2)) strength of silica fibre as a function of indentation load P.

decreases from 1000 to 100 $\mu m\,s^{-1}$, indicating that substantial fatigue is still occurring ($n \approx 35$). This is not surprising given that it is well known that water cannot be completely removed from the surface of silica without heating to elevated temperatures. This residual moisture explains at least some of the difference between the result in liquid and gaseous nitrogen.

The slope of the $\log\sigma_f$–$\log P$ plot in the post-threshold region is found to be $-0{\cdot}227 \pm 0{\cdot}025$ (95% confidence interval) which is significantly different from the value of $-\frac{1}{3}$ predicted by eqn. (2) and from previous observations at higher loads. The reason for this discrepancy is not clear but may relate to the fact that our data are concentrated near the threshold region. The post-threshold models may not hold accurately here. In particular, we have not observed well developed lateral cracks below loads of 10 N. Therefore the magnitude and distribution of the residual stresses will not scale simply with load in this region as is assumed by the Cook and Lawn (1984) model. In addition, the shape of the radial cracks differs substantially from the penny shape assumed by the model. Both of these effects would reduce the strength near the threshold below that expected by the model, thus lowering the slope of the $\log\sigma_f$–$\log P$ plot in this region.

The subthreshold data lie on a well defined straight line of slope $-0{\cdot}253 \pm 0{\cdot}019$ which is in close agreement with the value of $-\frac{1}{4}$ that we have predicted from the models of Jakus *et al.* and of Lathabai *et al.* for the initiation-controlled region far from the threshold. Given the narrow range of published data in this region, our data provide the first definitive confirmation of the $-\frac{1}{4}$ slope for subthreshold indents.

The slope of $-\frac{1}{4}$ is maintained up to the apparent threshold for the air indented data; there is no evidence for a propagation-controlled subthreshold region as predicted by Lathabai *et al.* (1991), since the behaviour does not curve downwards to the threshold. However, the extent of the propagation-controlled subthreshold regions is sensitive to the true value of P_c. Kurkjian, Kammlott and Chaudhri (1995) did not observe radial cracks for 10 N indentations made in liquid nitrogen. Lathabai *et al.* cite unpublished data also implying substantially higher values for P_c than observed for indents made in air (table 1). They suggest that 'post-threshold' air indentations close to the threshold are really subthreshold indentations that have popped in during unloading or very shortly thereafter owing to fatigue of the shear faults. Our data are consistent with this suggestion. A subthreshold propagation controlled regime that is collinear with the post-threshold region has been observed for other glasses by Lathabai *et al.* (1991). Our data preclude this behaviour for air indentations on silica when strength tested inert. However, if the strength of air indentations is measured under fatiguing conditions (e.g. dry nitrogen), which favour

Table 1. Various directly observed experimental parameters.

	a_{th} (μm)	P_c (N)	c_2^* (μm)	σ_I^0 (MPa)
Jakus *et al.* (1988)	16·6	3·9	24·6	—
Lathabai *et al.* (1991)	32·7	15	59	95·3
Kurkjian *et al.* (1995)	>27	>10	—	—
Current work, apparent value	14·6	3	27·5	337
Current work, assumed value	100	140	412·5	81·7

pop-in at lower applied stress, a propagation-controlled subthreshold region might be observed.

4.1. *Model fitting*

The subthreshold data in fig. 2 have been fitted by the Jakus *et al.* model, eqn. (3). Since there is no direct evidence for a propagation-controlled subthreshold region, a value of ϕ cannot be determined. Also, because the subthreshold region shows no curvature, it does not imply a value for a_{th}. Therefore a value of $a_{th} = 100\,\mu m (P_c = 140\,N)$ is assumed which, firstly, is consistent with the observations of Kurkjian *et al.* and, secondly, gives an almost straight line for fitting to the subthreshold data. Using values of $K_c \geqslant 0{\cdot}79\,MPa\,m^{1/2}$ and $H = 7\,GPa$, this gives $\Gamma = 79\,MPa$ and, by fitting, $\psi = 0{\cdot}21$. These parameters are summarized in table 2. Figure 3 shows the fitted curve, together with the prediction using the apparent $a_{th} = 14{\cdot}6\,\mu m$; the former fits the data well while the latter does not.

Table 2. Fit parameters of the subthreshold model of Jakus *et al.* (1988), eqns. (3) and (5).

	ψ	Γ (MPa)	ϕ (MPa)
Jakus *et al.* (1988)	0·3	194	211
Current work	0·21	79	—

Fig. 3

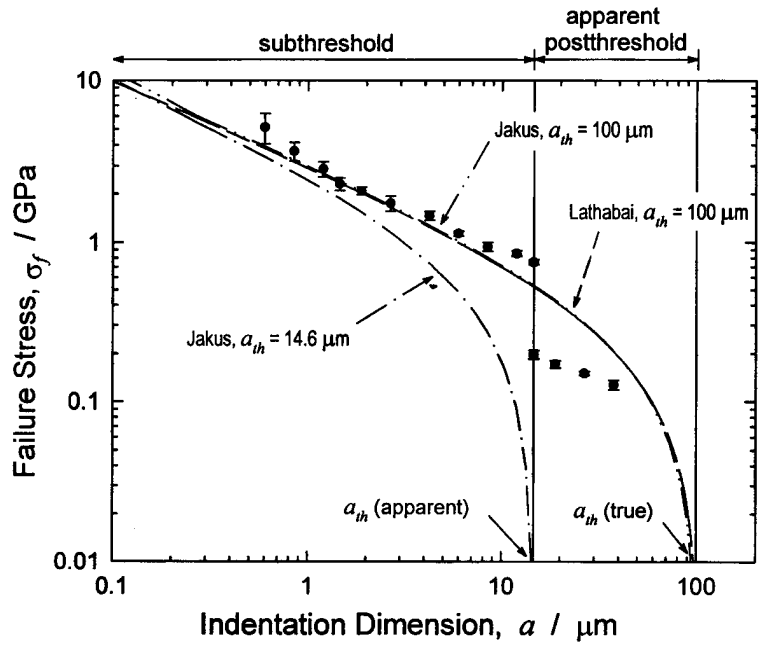

Inert (liquid-nitrogen) strength as a function of indentation size, compared with the Jakus *et al.* (1988) and Lathabai *et al.* (1991) subthreshold models.

The linearity of the subthreshold data means that the term containing Γ in eqn. (3) is small so that the subthreshold inert strength is the same as a simple Griffith flaw of size a without residual stress. Therefore the residual stresses do not influence the inert strength because they are small in comparison. However, under fatigue conditions, the strength is substantially lower and the residual stresses will be important and may have a significant detrimental impact on the reliability.

Table 3 shows values of the fit parameters for the Lathabai *et al.* model; again a_{th} is assumed to be 100 μm to ensure a constant slope of $-\frac{1}{4}$. The model using the fit values from table 3 is shown in fig. 3. and it is seen to almost exactly coincide with the Jakus *et al.* model. Although mathematically more complex, the Lathabai *et al.* model predicts essentially identical behaviour. The difference between the parameter values found for our data and by Lathabai *et al.* is mainly due to the overall higher strengths found in this work.

§ 5. Conclusions

We have described novel specimen handling and testing techniques that have permitted the inert liquid-nitrogen strength of fused silica fibre indented in air to be determined across a broad range of indentation loads which encompasses the threshold region for radial crack formation. The results have been compared with fracture mechanics models and are found to be in good agreement with their predictions, provided that it is assumed that the behaviour is well away from the true threshold for inert indentations. The models predict the existence of a propagation-controlled regime which has not been observed for fused silica. This is attributed to pop-in during or shortly after unloading of radial cracks from indents that would, in the absence of fatigue, have been subthreshold. The propagation-controlled regime might be observed if indentation is performed in an inert environment. The indentation environment is clearly important in determining the behaviour near the threshold.

The two fracture mechanics models considered are not experimentally distinguishable in this regime since they both predict essentially the same behaviour. The inert strength of the subthreshold indents can be simply modelled by a crack of a size equal to the indent size and assuming the residual stresses have negligible influence. However, the residual stress will be important when considering the long-term behaviour under a low applied stress in fatiguing environments when they are of comparable magnitude with the applied stress.

Acknowledgements

We thank Fiberguide Industries Inc. (Stirling, New Jersey) for donating optical fibre used in this study. This work was supported by the Fiber Optic Materials Research Program at Rutgers University and the New Jersey State Commission on Science and Technology.

Table 3. Fit parameters for the subthreshold model of Lathabai *et al.* (1991).

	α_R^T	α_R^S	α_A^T	α_A^S
Lathabai *et al.* (1991)	0·0524	0·0073	0·0084	0·0252
Current work	0·1862	0·0037	0·0030	0·0033

References

Aslanova, M. S., Baikova, L. G., Pukh, V. P., Sapozhkova, L. A., and Stepanov, M. I., 1982, *Fiz. Khim. Stekla*, **8**, 560.

Baikova, L. G., Pukh, V. P., and Talalakin, S. N., 1974, *Soviet Phys. solid St.*, **15**, 1437.

Breuls, T., and Svensson, T., 1993, *Fiber Optics Reliability and Testing: Benign and Adverse Environments*, Proceedings of SPIE, Vol. 2074 (Bellingham, Washington: SPIE), p. 78.

Choi, S. R., Ritter, J. E., and Jakus, K., 1990, *J. Am. Ceram. Soc.*, **73**, 268.

Cook, R. F., and Lawn, B. R., 1984, *Structural Reliability of Brittle Materials*, ASTM STP844, (Philadelphia, Pennsylvania: ASTM), p. 22.

Dabbs, T. P., and Lawn, B. R., 1985, *J. Am. Ceram. Soc.*, **68**, 563.

Dabbs, T. P., Marshall, D. B., and Lawn, B. R., 1980, *J. Am. Ceram. Soc.*, **63**, C224.

Glaesemann, G. S., 1992, *Proceedings of the 41st International Wire and Cable Symposium* (Eatontown: New Jersey: IWCS Inc.) p. 698.

Griffioen, W., 1994, *Opt. Engng.*, **33**, 488.

Gulati, S. T., 1992, *Photonics Spectra*, **26**, 78.

Jakus, K., Ritter, J. E., Choi, S. R., Lardner, T. J., and Lawn, B. R., 1988, *J. non-crystalline Solids*, **102**, 82.

Kurkjian, C. R., Biswas, D. R., and Yuce, H. H., 1996, *Optical Network Engineering and Integrity*, Proceedings of SPIE, Vol. 2611 (Bellingham, Washington: SPIE), p. 56.

Kurkjian, C. R., Kammlott, G. W., and Chaudhri, M. M., 1995, *J. Am. Ceram. Soc.*, **78**, 737.

Kurkjian, C. R., and Paek, U. C., 1983, *Appl. Phys. Lett.*, **42**, 251.

Lathabai, S., Rödel, J., Dabbs, T. P., and Lawn, B. R., 1991, *J. Mater. Sci.*, **26**, 2157.

Marshall, D. B., and Lawn, B. R., 1980, *J. Am. Ceram. Soc.*, **63**, 532.

Matthewson, M. J., Kurkjian, C. R., and Gulati, S. T., 1986, *J. Am. Ceram. Soc.*, **69**, 815.

Matthewson, M. J., Kurkjian, C. R., and Hamblin, J. R., 1996, *J. Lightwave Technol.*, submitted.

Nelson, G. J., Matthewson, M. J., and Lin, B., 1996, *J. Lightwave Technol.*, **14**, 555.

Wiederhorn, S. M., 1972, *J. Am. Ceram. Soc.*, **55**, 81.